Structure and Properties of Biaxial-Oriented Crystalline Polymers by Solid-State Crossrolling

Y. Yang,[1] J. Keum,[1] Z. Zhou,[1] G. Thompson,[2] A. Hiltner,[1] E. Baer[1]

[1]*Macromolecular Science and Engineering Department, Center for Applied Polymer Research (CAPRI), Case Western Reserve University, Cleveland, OH 44106-7202*
[2]*U.S. Army Dental and Trauma Research Detachment (USADTRD), Great Lakes, IL 60088-5259*

Received 20 November 2009; accepted 8 March 2010
DOI 10.1002/app.32414
Published online 24 May 2010 in Wiley InterScience (www.interscience.wiley.com).

ABSTRACT: The effect of biaxial orientation by solid-state crossrolling on the morphology of crystalline polymers including polypropylene (PP), high density polyethylene (HDPE) and Nylon 6/6 was investigated with polarized optical microscopy, atomic force microscopy, wide-angle X-ray scattering, and small-angle X-ray scattering techniques. It was found that crossrolling gradually changed the initial spherulitic structure into a biaxially oriented crystal texture with chain axis of crystals becoming parallel to the rolling direction for all three polymers. The effect of microstructure change on the macromechanical properties was studied in tension at both ambient temperature and −40°C. In tension at room temperature, the localized necking deformation of HDPE and PP control changed upon orientation into homogeneous deformation for the entire sample length. This was attributed to that the oriented crystal morphology eliminated the stress concentration, which existed in the original spherulitic structure from lamellae orientation in the polar and equatorial regions. At ambient conditions, the elastic moduli of HDPE and PP were found to decrease slightly with orientation whereas the modulus of Nylon 6/6 increased with increasing orientation. This was due to the fact that the amorphous chains of HDPE and PP are in a rubbery state and orientation increased the shear relaxation in the orientation direction but the amorphous chains of Nylon 6/6 are in the glassy state inhibited the shear relaxation. Both the yield stress and strain hardening exponent increased with increasing orientation for all three polymers. In tension at −40°C, orientation changed the failure mechanism of all three polymers from brittle fracture into ductile failure, as the original spherulitic structure was changed into an oriented structure with chain axis of crystals becoming parallel to the tension direction, which allowed chain slip deformation of crystals and resulted in oriented samples showing ductile failure. J Appl Polym Sci 118: 659–670, 2010

Key words: orientation; soilid-state structure; spherulites; morphology; mechanical properties

INTRODUCTION

When cooled from the melt, semicrystalline polymers like high density polyethylene (HDPE), polypropylene (PP), and Nylon 6/6 are known to form spherulites, which consist of radially oriented crystal lamellae and interlamellar amorphous regions. These crystalline polymers can be oriented by solid-state drawing, rolling, and compression. Solid-state orientation can lead to significant enhancement in properties when compared to orientation from the polymer melt, as the molecular chains in the solid-state have lower mobility thereby freezing in the overall orientation. During solid-state orientation of crystalline polymers, the initial isotropic spherulitic structure is destroyed by plastic deformation of the crystals and transforms into an anisotropic microfibrillar structure.[1–5] Deformation of the spherulitic structure of crystalline polymers under applied stress has been extensively studied in the literature.[2,6–13] However, because of the complicated microcomposite morphology of the spherulites and the existence of a variety of crystal forms, the solid-state deformation mechanisms are still not well understood. It is believed that early deformation is mainly in the amorphous phase consisting of interlamellar shear, lamellar separation, lamellar compression, and lamellar stack rotation. The deformation of amorphous chains is elastic and when exhausted will be followed by plastic deformation of crystals. Two major deformation mechanisms have been observed: chain slip and transverse slip. Twinning and martensitic transformation can also occur in some polymers; however, these mechanisms usually are minor components. Virtually all these deformation mechanisms are temperature dependent,[14] and studies of polyethylene deformation showed that interlamellar shear was enhanced at temperatures above 80°C,[15] whereas the martensitic transformation was suppressed.[16] Higher temperature increases both the number of dislocations generated and the mobility for chain slip deformation.[17]

Correspondence to: Y. Yang (yxy60@case.edu).

TABLE I
Summary of Crossrolled Polymers

Material designation		Original thickness (mm)	Thickness after crossrolling (mm)	Thickness reduction (%)
PP	Control	4.5	4.5	–
	50%	9.0	4.5	50
	75%	18.0	4.5	75
HDPE	Control	4.5	4.5	–
	50%	9.0	4.5	50
	75%	18.0	4.5	75
Nylon 6/6	Control	3.2	3.2	–
	50%	6.4	3.2	50
	75%	12.8	3.2	75

With increasing molecular orientation in the solid-state, the mechanical properties including modulus, yield stress, strain hardening, and fracture strength can be improved significantly. It was reported that the tensile strength of oriented PP by rolling can be improved by a factor of 10, and the modulus of HDPE and PP can be improved by a factor of 4 with a draw ratio of 10.[18,19] Another study showed that orientation significantly improved the low temperature impact toughness of PP because of the crack blunting mechanism.[20] This large improvement results from highly anisotropic structures. There still exists a lack of understanding, which relates the macroscopic mechanical properties to the oriented hierarchical morphology.

In this work, we studied the effect of biaxial orientation by crossrolling on the crystalline and amorphous phase morphology of three semicrystalline polymers (HDPE, PP, and Nylon 6/6). The mechanical properties under uniaxial tension of these oriented crystalline polymers are investigated at both ambient and low temperature conditions. Subsequently, the relationships between the oriented solid-state structure and mechanical behavior were established.

EXPERIMENTAL

Materials

Three semicrystalline polymers, PP, HDPE, and Nylon 6/6 were used in this study. Isotactic PP samples were commercially extruded sheets from Compression Polymers (Moosic, PA). HDPE sheets were prepared by compression molding pellets of a Ziegler–Natta polyethylene UNIVAL® DMDH-6400 from Dow Chemical Company (Freeport, TX) at 190°C with a Model 3912 Carver laboratory press (Wabash, IN). Nylon 6/6 sheets were commercially extruded sheets from Quadrant Engineering Plastics Products (Reading, PA). The polymer sheets were biaxial oriented by a crossrolling technique, which has been described in a previous study.[21] Table I gives the crossrolling material matrix. Both HDPE and PP sheets were crossrolled at ambient temperature whereas the Nylon 6/6 sheets were heated to 100°C before crossrolling. Different degrees of orientation were achieved by crossrolling the sheets to different thickness reductions of 50 and 75%. Samples with 50% thickness reduction had an equal biaxial draw ratio of 1.4 × 1.4, and samples with 75% thickness reduction had an equal biaxial draw ratio of 2.0 ×

TABLE II
List of Polymer Properties Before and After Crossrolling

Material designation		Melting point (°C)	Crystallinity (%)[a]	Amorphous fraction (%)[b]	Water absorption (%)	T_g (°C)
PP	Control	158	43	60	–	~0
	50%	159	41	57		
	75%	157	40	58		
HDPE	Control	134	75	36	–	<−76[c]
	50%	134	72	46		
	75%	133	69	57		
Nylon 6/6	Control	260	31	70	1.2	~50
	50%	261	35	70	0.9	
	75%	262	36	65	0.6	

[a] Crystallinity is calculated from DSC measurement.
[b] Amorphous content determined from WAXS measurement.
[c] Value listed as brittle temperature on manufacturer's datasheet.

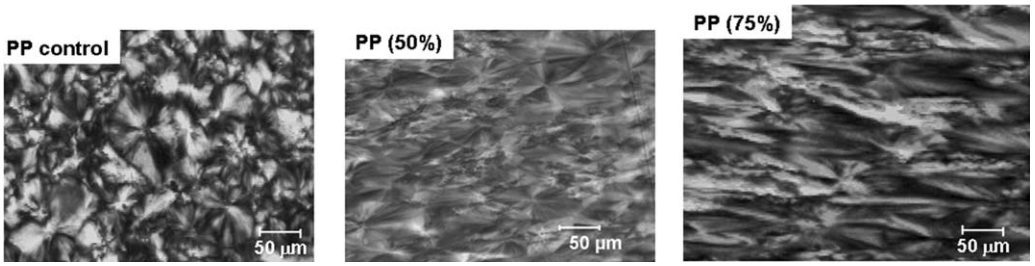

Figure 1 Effect of orientation on the spherulitic morphology of polypropylene characterized by polarized optical microscopy from the side-view.

2.0. The HDPE and PP sheets were 4.5 mm thick after crossrolling and the Nylon 6/6 sheets were 3.2 mm thick after crossrolling. An unoriented sheet with the same thickness was used as the control for this study. Table II lists various properties of the three polymers before and after crossrolling.

Polarized optical microscopy and atomic force microscopy

The effect of crossrolling on the morphology of PP was examined by polarized optical microscopy using an Olympus (Lake Success , NY) BH-2 optical microscope. Thin films of about 1-μm thick were sliced in the cross section with a ultramicrotome (MT6000-XL from RMC, Tucson, AZ) then placed between two glass slides for the polarized optical microscopy observation. In the case of HDPE and Nylon 6/6, we used atomic force microscopy (AFM) because the dimensions of spherulites were too small to detect using polarized optical microscopy. Cross sections with thickness of 200 nm were microtomed in the thickness direction at −95°C for HDPE and −55°C for Nylon 6/6. Both phase and height images of the cross sections were recorded simultaneously at ambient temperature in air using the tapping mode of the Nanoscope IIIa MultiMode scanning probe (Digital Instruments, Santa Barbara, CA).

Wide-angle X-ray scattering and small-angle X-ray scattering

The structure and global orientation of the crossrolled polymer sheets were examined by two-dimensional (2D) wide-angle X-ray scattering (WAXS) and small-angle X-ray scattering (SAXS) measurements using an in-house set-up with rotating anode X-ray generator (Rigaku RU 300, 12 kW). To collect 2D WAXS images, collimated X-ray beam with 1 mm diameter was irradiated in the direction parallel to the rolling direction (RD) or the normal direction (ND) of polymer sheets and the scattered beam was recorded using Bruker Hi-Star detector. 2D SAXS were collected using a Rigaku S-Max3000 pinhole camera, which gives a highly focused parallel beam of monochromatic Cu Kα radiation ($\lambda = 0.154$ nm) and equipped with a 2D gas filled multiwire detector. The X-ray exposure time was 20 min for WAXS and 30 min for SAXS. Because samples were equally oriented in two crossrolling directions, and the WAXS and SAXS images measured along the two rolling directions were identical to each other without discernable differences, only one of the two RD X-ray patterns are shown.

Tension test

The uniaxial tension experiments were conducted on an MTS Alliance RT30 using ASTM D1708 test specimens. The dimension of the specimens were 50 × 6.5 × 4.5 mm ($L \times W \times T$) for HDPE and PP and 50 × 6.5 × 3.2 mm for Nylon 6/6. Tension tests were conducted at both ambient condition and −40°C with a strain rate of 1%/min. For ambient tension tests, a square grid pattern of 30 wires per inch was created by depositing 200 Å gold coating onto the specimens to determine the true stress-true strain. The specimen deformation was photographed with an Olympus C-5050ZOOM digital camera, and from this information true strain and true stress were obtained. For low temperature tension test, the specimen was first put into an environmental chamber and cooled to the set temperature of −40°C. After the set temperature was reached, it was allowed to further equilibrate for 15 more minutes before the test was started.

RESULTS AND DISCUSSION

Orientation characterization with polarized optical microscopy and atomic force microscopy

The deformation of spherulites of PP shown in Figure 1 was studied by polarized optical microscopy from the side-view parallel to the RD. For HDPE and Nylon 6/6, as their spherulites are relatively small, AFM was used to observe spherulitic morphology changes under crossrolling conditions. These results are shown in Figures 2 and 3.

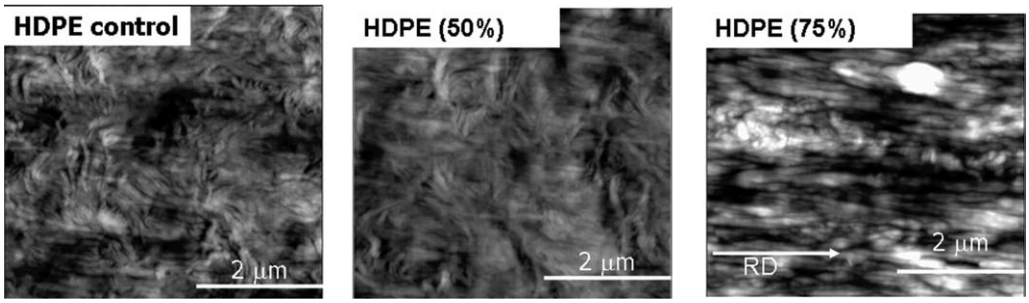

Figure 2 Effect of orientation on the spherulitic morphology of HDPE characterized by atomic force microscopy (AFM): left to right direction is the sample rolling deformation direction and top to bottom is the sample thickness direction.

In Figure 1, the unoriented control shows spherulitic structure with diameter of spherulites around 100 μm. With 50% thickness reduction, the spherulites were seen to be deformed into an elliptical shape with the long axis of the ellipse being in the rolling direction and the short axis in the thickness direction as the spherulites were stretched in the rolling direction and compressed in the thickness direction. When the sample was crossrolled even more down to 75% in thickness reduction, the spherulites became more elongated in the rolling direction to about 3–4 times of its original length and more flattened in the thickness direction to form a disc-like structure. The spherulite boundary now became barely discernable at this level of thickness reduction.

The morphology change with crossrolling of HDPE is depicted in Figure 2. It was shown by AFM that the HDPE control also exhibited a spherultic morphology. At 50% crossrolling thickness reduction, crystalline textures were aligned along the rolling direction and, with further thickness reduction to 75%, more oriented crystalline texture was seen in the AFM height image.

Similarly, the effect of crossrolling deformation on the spherulitic morphology of Nylon 6/6 was also studied using AFM, Figure 3. The spherulite dimensions were smaller than PP. These spherulites were also stretched in the rolling direction at 50% crossrolling thickness reduction and the spherulitic boundary can still be observed. With 75% rolling thickness reduction, the spherulites were deformed even more and the spherulite boundary can no longer be observed.

2D Wide-angle X-ray scattering and 2D small-angle X-ray scattering

The effect of crossrolling on both the crystalline lamellae and amorphous chain orientation was examined by 2D WAXS and SAXS. Figure 4(a) compares the 2D WAXS patterns of PP at different crossrolling thickness reductions with X-ray beam parallel to the rolling plane of the sample. Isotropic ring reflections from monoclinic (α-form) crystal planes, i.e., (110), (040), (130), and (111/041), were observed for PP control, indicating the random distribution of crystals in the spherulite.[22] The random distribution of lamellar crystals can be further confirmed by the 2D SAXS pattern, which is given in Figure 4(b). The SAXS pattern of PP control exhibited a ring-like scattering pattern, inferring no preferred orientation of lamellar crystals. The long period (L_p) of lamellar stack obtained from the maximum of first order scattering was about 16 nm. At 50% thickness reduction, the 2D WAXS pattern revealed 4-arc reflections from (110), (040), and (130) crystal planes at the off-axes and the (111/041) reflections at the equatorial and

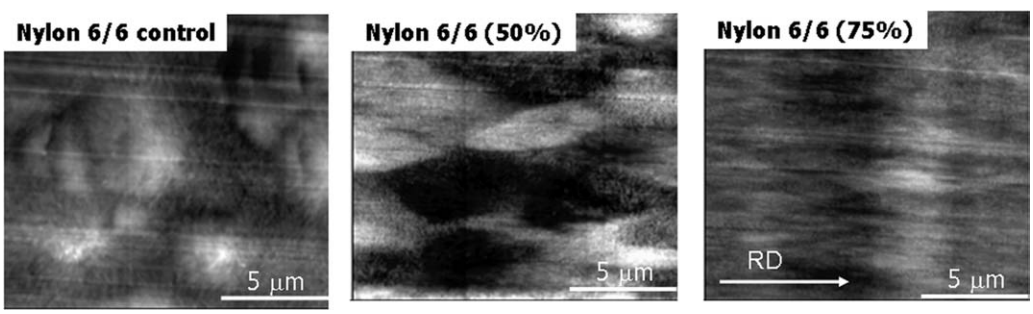

Figure 3 Effect of orientation on the spherulitic morphology of Nylon 6/6 characterized by atomic force microscopy (AFM): left to right direction is the sample rolling deformation direction and top to bottom is the sample thickness direction.

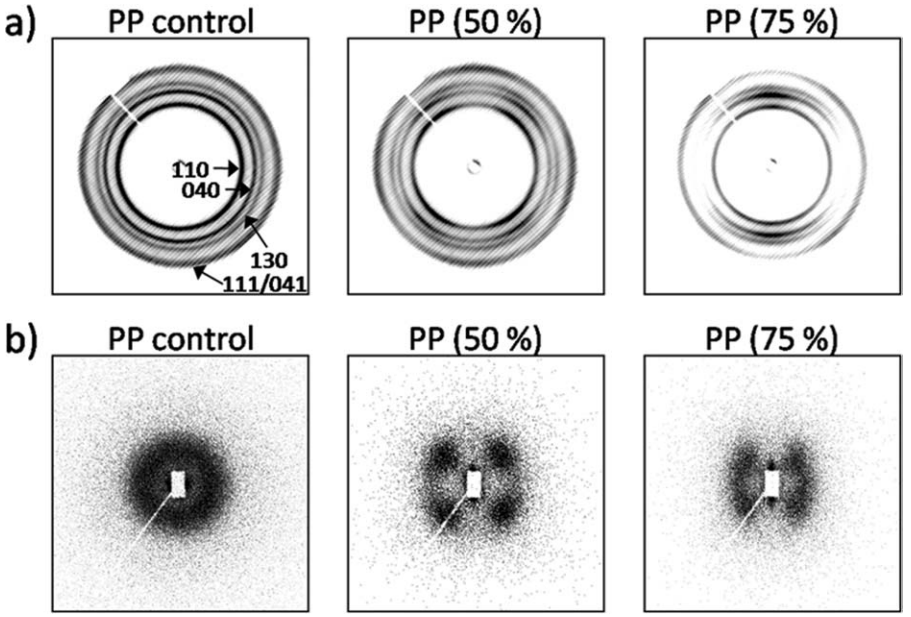

Figure 4 Two-dimensional (2D) WAXS (a) and 2D SAXS (b) patterns of crossrolling biaxial oriented PP sheets from side-view. The X-ray beam was aligned parallel to the plane of sheets and the crossrolling direction was horizontal in the X-ray images. The amount of thickness reduction and the Miller indices are indicated.

polar direction. This showed that the crystals were tilted to RD during orientation. In SAXS, 4-point pattern was observed at azimuthal angles around 45°, 135°, 225°, and 315°, and L_p remained almost identical to the value in the unoriented control. The 4-point SAXS and 4-arc WAXS patterns indicated that the lamellae were tilted about 45° to RD. This lamellae first become tilted to the deformation direction has been previously observed in the literature.[23] It was suggested that this was due to lamellae kinking to form a chevronlike lamellar structure. As the thickness reduction of PP was further increased to 75%, the WAXS pattern showed 2-arc reflections of (110), (040), and (130) at the polar direction and 4-arcs (111/041) reflection at the off-axis. This indicated that the PP crystallites were further oriented with the *c*-axis of the crystals becoming aligned along the RD. Because of the increased thickness reduction, the azimuthal angles of the 4-point SAXS pattern were further moved to 30°, 150°, 210°, and 330°. Because the chain axis in lamellae at 75% thickness reduction was predominantly aligned along RD as seen in Figure 4(a), the 4-point SAXS pattern must be related to the tilted periodic arrangement of fragmented lamellae. Base on the azimuthal angles of 4-point scattering, we concluded that the fragmented lamellae were periodically arranged with the angle of about ±60° from RD. L_p at 75% thickness reduction sample was changed to about 18 nm due to deformation of amorphous phase. Because the crystal lamellar thickness did not change during crossrolling, the increased L_p was attributed to the stretching of amorphous phase thereby increasing the distance between the lamellar stacks. In the SAXS pattern of PP with 50% and 75% thickness reduction, a polar scattering streak was observed close to the X-ray beam stop. This was attributed to the formation of microvoids and/or microfibrils, which were oriented parallel to RD.[24] The normal direction WAXS and SAXS patterns were shown in Figure 5. It was seen that the spherulitic structure in the rolling plane was maintained. Based on the polarized optical microscopy observation of spherulite deformation and 2D WAXS and SAXS examination of lamellae orientation, a schematic of the morphology change with crossrolling is given in Figure 6.

Figure 7(a,b) showed the WAXS and SAXS characterization of lamellae orientation of HDPE. In Figure 7(a), the 2D WAXS pattern of HDPE control shows isotropic reflection rings from orthorhombic (110) and (200) crystal planes indicating a random distribution of crystals.[25] The isotropic ring-like SAXS pattern of HDPE control in Figure 7(b) confirmed the random orientation of lamellae in the control. The L_p obtained from the 2D SAXS pattern was about 30 nm. As the HDPE control was crossrolled to 50% thickness reduction, the WAXS pattern exhibited broad six-arc (110) and (200) reflections at the pole and off-axis. The 2-arc polar reflections are related to lamellae with chain axis being parallel to the rolling direction and the 4-arc off-axis reflection is the result of {310} twinning on unloading after the sample was deformed by rolling deformation.[23] At 50% thickness reduction, the ring-like SAXS pattern of HDPE control was changed to

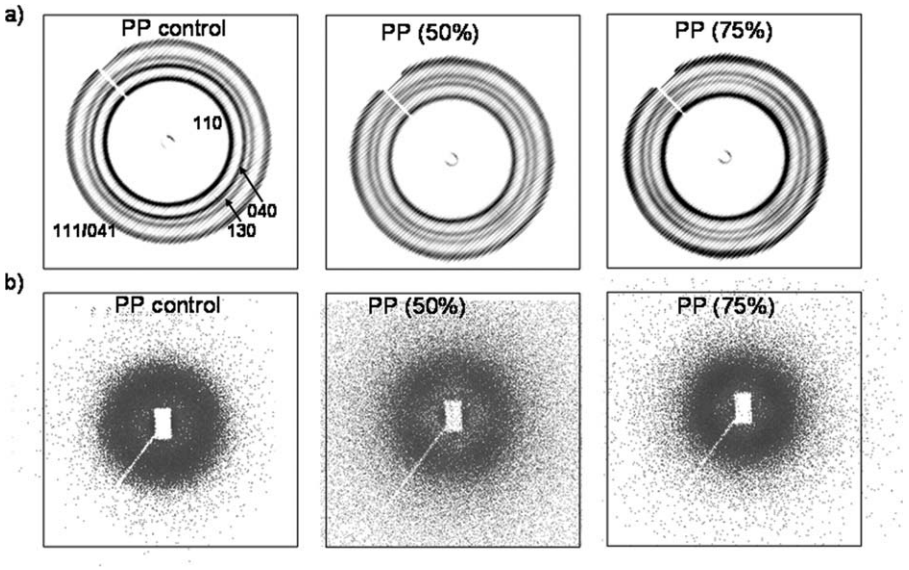

Figure 5 Two-dimensional (2D) WAXS (a) and 2D SAXS (b) patterns of crossrolling biaxial oriented PP sheets from top-view. The X-ray beam was aligned parallel to the plane of sheets and the crossrolling direction was horizontal in the X-ray images. The amount of thickness reduction are and the Miller indices are indicated.

a very weak oval shaped pattern overlapped by a strong 4-point pattern. The oval shape of SAXS pattern was related to the different deformation mechanisms of the amorphous phase in a spherulite. In the polar region of a spherulite, the deformation mechanism of amorphous phase is interlamellar separation, however, the deformation of amorphous phase in equatorial region is interlamellar shear and contraction. This leads to the oval shape SAXS pattern with shorter axis (longer L_p) at the equator and longer axis (shorter L_p) at the pole. The 4-point SAXS pattern is due to tilted lamellar stacks and fragmented lamellar blocks, periodically arranged with an angle to the RD. The L_p at the maximum intensity point was about 33 nm due to the stretching of amorphous chains. With thickness reduction increased further to 75%, the reflection arcs of (110) and (200) became sharper in azimuthal distribution. Also the 2-arc polar (110) reflection became stronger in intensity whereas the 4-arc off-axis (110) reflection became weaker. This implied that by further crossrolling more lamellae had become aligned parallel to the RD. In addition, a weak two-arc meridianal reflection emerged inside the (110) reflections at 50% thickness reduction, which became more discernable at 75% thickness reduction. This reflection is related to the martensitic transformation, corresponding to the conversion of orthorhombic to monoclinic crystal in PE.[26,11] In Figure 7(b), the oval shaped SAXS pattern became even weaker in intensity whereas the 4-point pattern became stronger for HDPE with 75% thickness reduction. The L_p in the maximum intensity point remained at about 33 nm. These results suggested that more lamellae became tilted or fragmented and aligned along the rolling direction.

In Figure 8(a), the 2D WAXS pattern of Nylon 6/6 control exhibited isotropic reflection rings from (100) and (010/110) crystal planes corresponding to the random orientation of α (triclinic) crystals of Nylon 6/6.[27,28] The ring-like SAXS pattern in Figure 8(b) showed isotropic spherulitic morphology of the control. The L_p of Nylon 6/6 control was determined to be about 10 nm. At 50% thickness reduction, the ring-like (010/110) WAXS reflection was transformed to a 2-arc pattern at the polar region. This implied that the crystallographic *b*-axis and the reciprocal lattice vector of (110) crystal plane were parallel to the normal direction of the sheet. This suggests that the *c*-axis in crystals was aligned along RD by the crossrolling. Because the angle between crystallographic *b*- and *a*-axis in triclinic unit cell of Nylon 6/6 is ~63°,[27,28] (100) crystal plane appeared at the off-axis, $\varphi = 27°$. The SAXS pattern showing 4-point pattern at azimuthal angles of 64°, 116°, 244°, and 296° was due to the tilted lamallar stacking or the periodic arrangement of fragmented

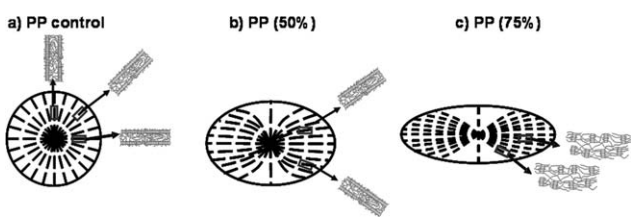

Figure 6 Schematic of spherulite and lamallar deformation with crossrolling: (a) PP control, (b) PP(50%), and (c) PP(75%).

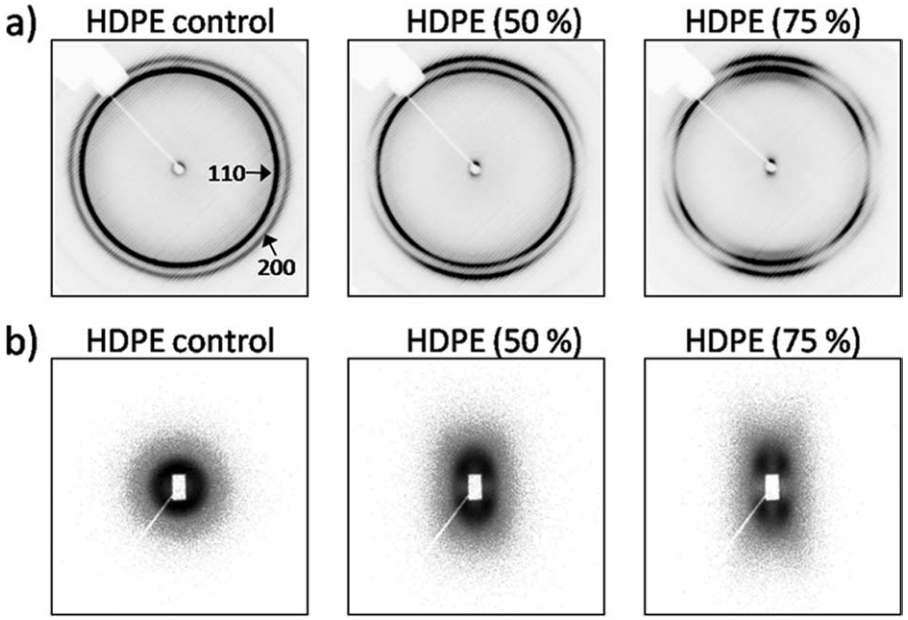

Figure 7 2D WAXS (a) and 2D SAXS (b) patterns of HDPE sheets. The X-ray beam was aligned parallel to the plane of sheets and the crossrolling direction was horizontal in the X-ray images. The amount of thickness reduction and the Miller indices are as indicated.

lamellae. L_p at the maximum scattering point was increased to about 12 nm due to the stretching of the amorphous chains. At 75% thickness reduction, the azimuthal distribution of (010/110) reflection became narrower due to increase in orientation. The azimuthal angles of 4-point SAXS pattern were 56°, 124°, 236°, and 304°, indicating further orientation of lamellae. The L_p was decreased to about 7 nm, which is probably due to lamellar fragmentation into smaller crystal blocks. The increased population of crystal blocks could result in the decreased distance between the crystallites.

Effect of orientation on uniaxial tensile behavior at ambient temperature

The effect of crossrolling on the mechanical properties of PP, HDPE, and Nylon 6/6 was studied in uniaxial

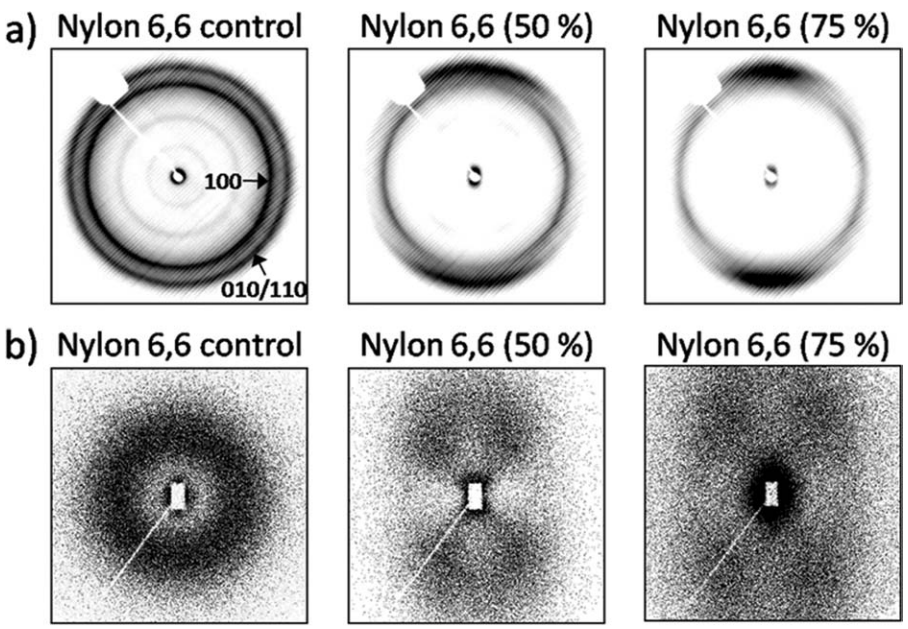

Figure 8 2D WAXS (a) and 2D SAXS (b) patterns of Nylon 6/6 sheets. The X-ray beam was aligned parallel to the plane of sheets and the crossrolling direction was horizontal in the X-ray images. The amount of thickness reduction and the Miller indices are as indicated.

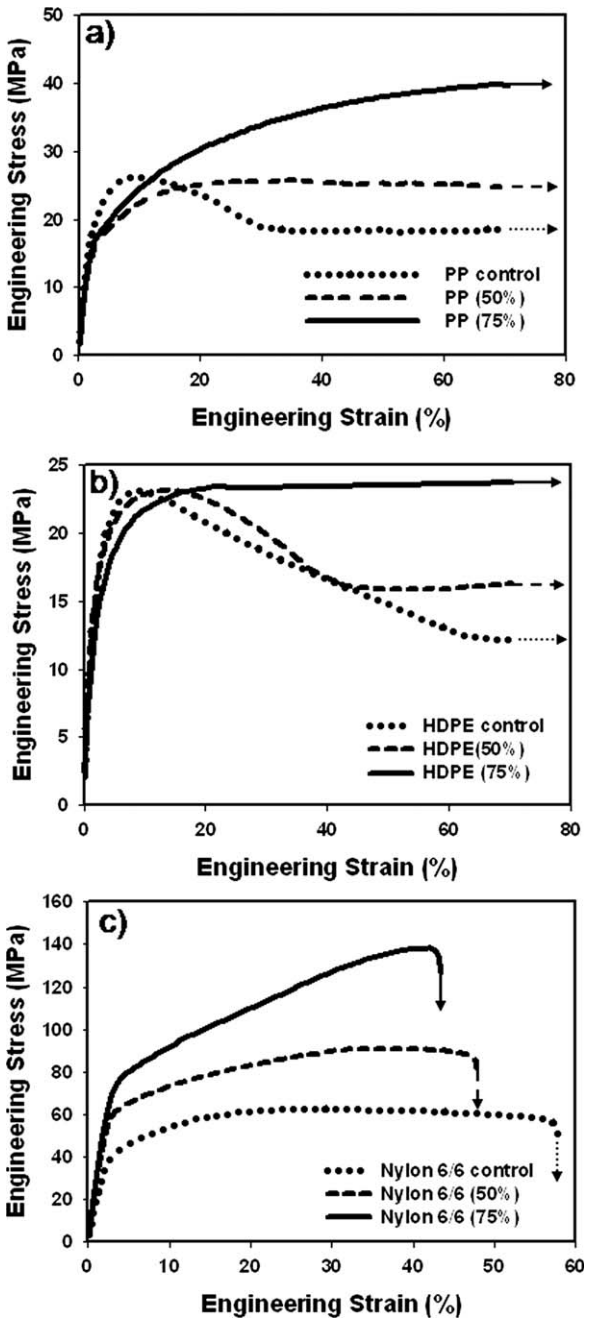

Figure 9 Effect of orientation on the tensile engineering stress-engineering strain behavior at ambient conditions: (a) PP, (b) HDPE, and (c) Nylon 6/6. The horizontal arrows indicate that the sample didn't fail at that strain and the vertical arrows indicate the strain of which the sample fractured.

tension at room temperature, which is above the T_g of HDPE and PP but below the T_g of Nylon 6/6. Figure 9(a–c) compare the effect of crossrolling on their respective engineering stress-strain curves. In Figure 9(a), the engineering stress-strain curve of PP control shows localized necking deformation at the yield stress. With increasing strain, the stress decreases and becomes nearly constant stress in the draw region. However, in both PP (50%) and PP (75%) oriented samples, no necking was observed indicating a "homogeneous deformation" for the whole sample length. Inhomogeneous necking deformation of crystalline polymers is associated with the highly localized plastic deformation of crystals. The spherulitic structure is transformed into a microfibrillar structure by lamellar fragmentation followed by rearrangement of crystal blocks. In the polar regions of a spherulite, the chain axis of crystals are perpendicular to the

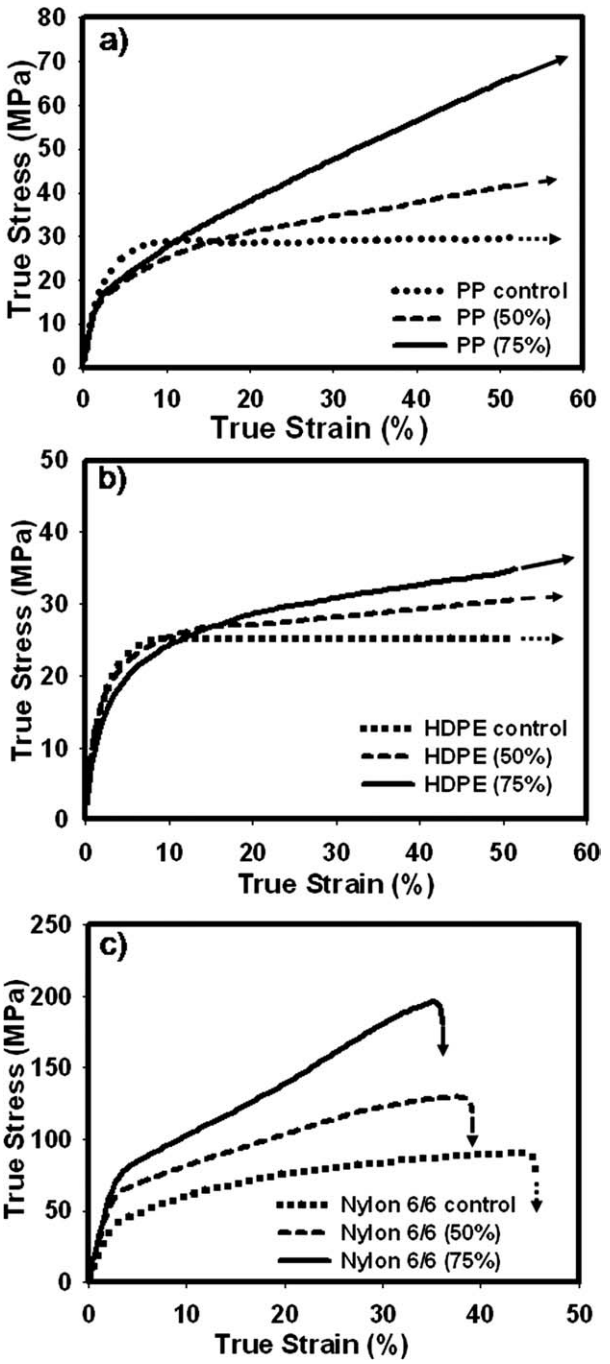

Figure 10 Effect of orientation on the tensile true stress-true strain behavior at ambient condition: (a) PP, (b) HDPE, and (c) Nylon 6/6.

TABLE III
Effect of Orientation on the Mechanical Properties in Uniaxial Tension at Room Temperature and −40°C

Material		Ambient condition tension			−40°C tension	
		E (MPa)	σ_y (MPa)	n	E (MPa)	σ_y (MPa)
PP	control	1100 ± 30	26 ± 1	0	2300 ± 60	46 ± 2
	50%	1000 ± 80	27 ± 1	0.07 ± 0.01	2400 ± 70	52 ± 2
	75%	900 ± 40	29 ± 1	0.16 ± 0.01	2500 ± 100	66 ± 1
HDPE	control	1130 ± 30	26 ± 1	0	3000 ± 60	62 ± 2
	50%	1020 ± 30	28 ± 1	0.15 ± 0.02	3200 ± 50	67 ± 4
	75%	970 ± 50	30 ± 1	0.34 ± 0.02	3650 ± 80	72 ± 2
Nylon 6/6	control	1900 ± 100	46 ± 1	0.28 ± 0.02	3300 ± 50	122 ± 2
	50%	2670 ± 120	67 ± 4	0.41 ± 0.03	3400 ± 100	142 ± 2
	75%	2860 ± 220	83 ± 5	0.60 ± 0.06	3600 ± 80	153 ± 3

tensile direction [Fig. 6(a)] resulting a greater deformation resistance than crystals in the equatorial regions with chain axis parallel to the tensile direction.[2,8] As a result stress concentration leads to localized necking deformation for unoriented PP control. With crossrolling, the lamellae are tilted and with increasing thickness reduction are further aligned along the rolling direction [Fig. 6(b,c)]. This lamellar alignment along the rolling direction explains suppression of necking in the uniaxial tension.

Figure 9(b) shows the effect of crossrolling on the engineering stress-strain curve of HDPE. Like PP control, unoriented HDPE control also exhibited necking and a yield maxima. However, unlike PP, HDPE (50%) still showed localized yielding. This was due to remnants of lamellae in the polar region as evidenced in the SAXS pattern [Fig. 7(b)]. For HDPE (75%), homogeneous deformation was observed without necking since as before spherulitic structure was now modified into tilted and parallel lamellae along the tension direction.

The engineering stress-strain curve comparison for Nylon 6/6 with different degrees of crossrolling is given in Figure 9(c). For Nylon 6/6, all three samples showed homogenous deformation without necking. The is probably due to the lower crystallinity of Nylon 6/6. It has been shown that necking is related to high crystallinity.[3,29,30] For low crystallinity polymers, the majority of the deformation will occur in the amorphous phase.

Inhomogeneous necking deformation prevents the calculation of true stress and true strain in a specimen, which can only be obtained by measuring the localized deformation area. Figure 10(a–c) compare the true stress-true strain curves of PP, HDPE, and Nylon 6/6 at different degrees of crossrolling. At low strains, Hooke's law applies in the elastic region: $\sigma = E\varepsilon$, where σ is true stress, ε is true strain and E is the elastic modulus. In the plastic region, the true stress-true strain relation can be described by the power law model: $\sigma = K\,(\varepsilon\text{-}\varepsilon_y)^n$, where ε_y is the strain at yield and n is the strain hardening exponent[31,32] The elastic modulus was found to slightly decrease with orientation for HDPE and PP. However, it increased with increasing orientation for Nylon 6/6. This decrease of elastic modulus with orientation at small draw ratios has been observed by Ward,[1] who attributed it to the shear relaxation parallel to the c-axes of the crystallites. However, for Nylon 6/6, as its glass transition temperature is above the room temperature, the shear relaxation is no longer effective and thus the modulus increases with orientation.

The effect of orientation on the yield stress of the three polymers is given in Table III. For HDPE and PP, the yield stress showed only slight increase with orientation. However, the yield stress of 75% oriented Nylon 6/6 increased by 50% when compared to the unoriented control. For crystalline polymers, yielding is associated with the onset of plastic deformation of crystals.[33,34] Before yielding, the deformation is due to the stretching of amorphous chains. For HDPE and PP, their glass transition temperature is below room temperature so the amorphous chains are in a rubbery state and can be easily stretched. As a result, the yield stress exhibited only a small increase with orientation. For Nylon 6/6, as its glass transition temperature is above room temperature, the amorphous chains are in a glassy state, and consequently stretching the glassy amorphous chains requires much higher stress resulting in a larger increase in the yield stress with orientation.

The strain hardening exponent was determined from the linear fit of the slope of log σ against log ε plot for the plastic region of the true stress-true strain curve. The results are compared in Table III. It was found that the strain hardening exponent of all the crystalline polymers increased with orientation. The strain hardening of polymers is associated with the straightening or orientation of the network of chain entanglements.[3,4,9] Van Melick et al.[35] showed that increasing the density of the network and decreasing the chain mobility will increase the strain hardening exponent. Crossrolling has destroyed the

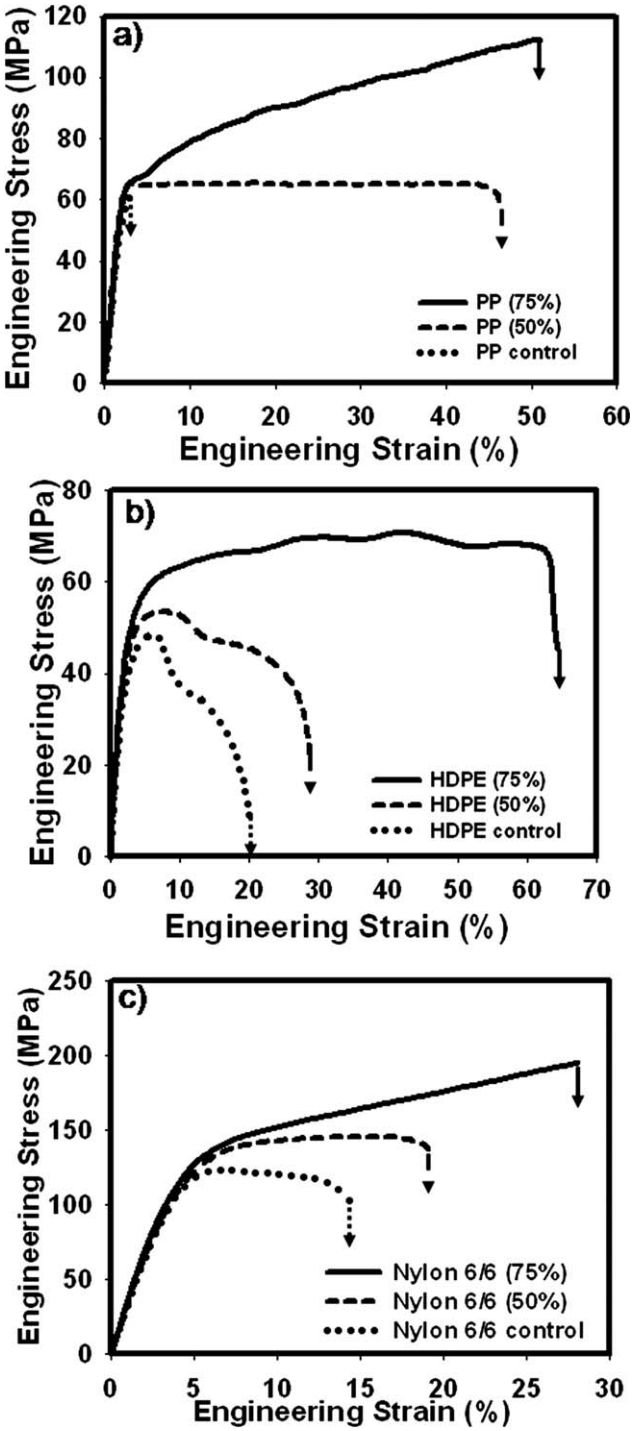

Figure 11 Effect of orientation on tensile engineering stress-strain behavior at −40°C: (a) PP, (b) HDPE, and (c) Nylon 6/6. The vertical arrows indicate the strain at which the sample fractured.

isotropic spherulitic structure and formed an oriented microfibril structure with the chain entanglement network stretched more with increasing crossrolling deformation. This explains the increased strain hardening exponent with increasing crossrolling deformation.

Effect of orientation on uniaxial tensile behavior at low temperature

The deformation of amorphous phase and lamellae crystals is affected by temperature especially below the T_g. It is well known that polymer chains will be changed from rubbery state to glassy state when the temperature is lowered to below T_g, which will greatly hinder the deformation of amorphous chains. For deformation of crystals, it can both reduce the number of dislocations and chain mobility for slip deformation. Figure 11(a–c) compares the engineering stress-strain curves at −40°C of PP, HDPE, and Nylon 6/6 with different amounts of crossrolling. In Figure 11(a), unoriented PP control showed brittle fracture without any plastic deformation. This was because the test temperature is below the T_g of PP and the amorphous chains are in glassy state inhibiting the rotation of lamellar stacks. However, ductile failure with large plastic deformation was observed for oriented PP(50%) and PP(75%). The fragmented lamellae are oriented with chain axis of crystals tilted or parallel to the tension direction allowing chain slip deformation of crystals along the tension direction resulting in improved ductility in both oriented PP(50%) and PP(75%) samples.

Figure 11(b) compares engineering stress-strain curve of HDPE with different crossrolling degrees at −40°C. Both HDPE control and HDPE (50%) exhibited necking type yielding. However, the necking did not propagate resulting in sample fracture with relatively small plastic deformation. For HDPE, the test temperature is around its T_g and plastic deformation of lamellae in the equatorial region with chain axis parallel to the tension direction is still allowed by chain slip deformation mechanism (Fig. 12), resulting in the necking type yielding. However, for lamellae in the polar region of the spherulites, the chain axes of molecules are perpendicular to the tension direction and they can only be deformed by transverse slip or "micronecking" (Fig. 12).[36] Near the T_g, the chain mobility is greatly reduced inhibiting the transverse slip deformation of lamellae in the polar region. The spherulitic structure of unoriented HDPE control was changed into a microfibrillar structure with chain axis of lamellae or fragmented lamellae being tilted or parallel to the rolling direction for HDPE (75%), which allowed large plastic deformation of crystals by chain slip deformation mechanism resulting in ductile failure.

Similar results were also observed for Nylon 6/6 [Fig. 11(c)]. The unoriented controls failed in a relatively brittle manner whereas the oriented samples showed improved ductility. Low strain fracture of Nylon 6/6 control can also be attributed to the test temperature being lower than its T_g, which limited the rotation of lamellar stacks. The larger fracture strain of Nylon 6/6 control when compared to PP is

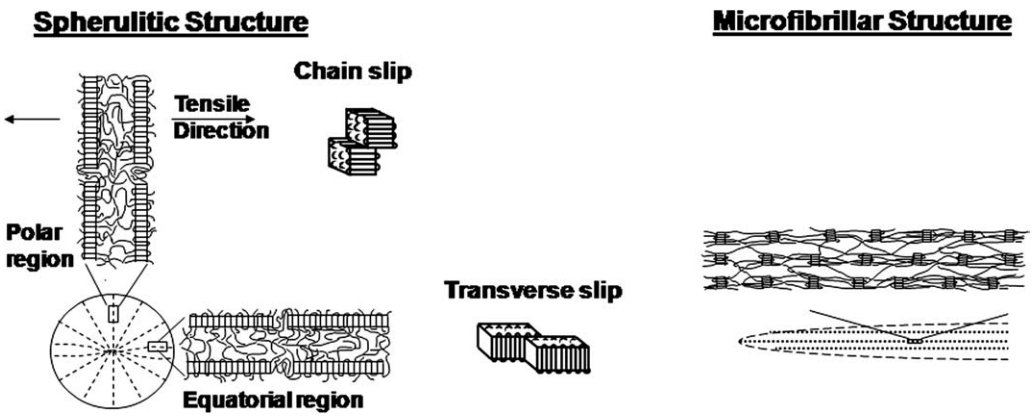

Figure 12 Schematic of different crystal deformation mechanism for equatorial and polar lamellae in spherulites: (a) chain slip for lamellae in the equatorial region, (b) transverse slip in the polar region.

probably due to its lower crystallinity and larger elastic deformation of the amorphous chains prior to fracture. Again with orientation, chain slip deformation of crystals was possible resulting in improved ductility for both oriented Nylon 6/6 (50%) and Nylon 6/6 (75%).

The effect of orientation on the elastic modulus and yield stress at low temperature were compared in Table III. Unlike the tension test at ambient condition, the modulus of all three polymers increased with increasing orientation because low temperature suppressed the shear relaxation. The yield stress of HDPE and PP from low temperature tension test showed a larger increase with orientation than that of room temperature. This is probably due to the fact that stretched amorphous chains are much stiffer at low temperature.

CONCLUSIONS

Biaxial orientation of crystalline polymers PP, HDPE, and Nylon 6/6 by solid-state crossrolling changed the initial spherulitic structure of the controls into an elliptical structure with long axis in the rolling deformation direction and short axis in the normal direction. The randomly distributed lamellae in the spherulitic structure were oriented by lamellar stack rotation, lamellar fragmentation, and rearrangement of fragmented lamellae into a crystal texture with chain axis becoming parallel to the rolling direction. This morphology change eliminated the stress concentration that existed in the unoriented spherulitic structure and localized necking deformation that was observed in the control samples was transformed into homogeneous deformation in the oriented sample in uniaxial tension at room temperature. The moduli of PP and HDPE decreased slightly with orientation but increased with orientation for Nylon 6/6. This was attributed to shear relaxation of chains above T_g in the orientation direction for both PP and HDPE. Orientation increased the yield stress and strain hardening exponent of all three semicrystalline polymers, which was attributed to stretching of the chain entanglement network during crossrolling deformation. At $-40^{\circ}C$, orientation changed the failure mechanism of all three polymers from brittle fracture into ductile failure as the morphology was changed from spherulitic structure to fragmented lamellae with chain axis of crystals parallel to the tension direction and allowed chain slip deformation of crystals. The elastic moduli of all three polymers increased with increasing orientation at $-40^{\circ}C$ as the shear relaxation in the chain axis direction was suppressed at low temperature.

References

1. Wards, I. M. Structure and Properties of Oriented Polymers; Chapman & Hall: New York, 1997.
2. Peterlin, A. J Mater Sci 1971, 6, 490.
3. Hiss, R.; Hobeika, S.; Lynn, C.; Strobl, G. Macromolecules 1999, 32, 4390.
4. Men, Y.; Strobl, G. Macromolecules 2003, 36, 1889.
5. Nikolov, S.; Lebensohn, R.; Raabe, D. J Mech Phys Solids 2006, 54, 1350.
6. Hay, I.; Keller, A.; Kolloid, Z. Polymer 1965, 204, 43.
7. Galeski, A.; Bartczak, Z.; Argon, A.; Cohen, R. Macromolecules 1992, 25, 5705.
8. Lin, L.; Argon, A. J Mater Sci 1994, 29, 294.
9. Pluta, M.; Bartczak, Z.; Galesk, A. Polymer 2000, 41, 2271.
10. Bartcak, Z.; Lezak, E. Polymer 2005, 46, 6050.
11. Pawlak, A.; Galeski, A. Macromolecules 2005, 38, 9688.
12. Zuo, F.; Keum, J.; Chen, X.; Hsiao, B.; Chen, H.; Lai, S.; Wevers, R.; Li, J. Polymer 2007, 48, 6867.
13. Galesk, A.; Argon, A.; Cohen, R. Macromolecules 1988, 21, 2761.
14. Butler, M.; Donald, A. Macromolecules 1998, 31, 6234.
15. Keller, A.; Pope, D. J Mater Sci 1971, 6, 453.
16. Kiho, H.; Peterlin, A.; Geil, P. J Polym Sci 1965, 3, 157.
17. Crist, B.; Fisher, C.; Howard, P. Macromolecules 1989, 33, 1709.
18. Bartczak, Z.; Morawiec, J.; Galeski, A. J Appl Polym Sci 2002, 86, 1413.
19. Ajji, A.; Legros, N.; Dumoulin, M. Adv Perform Mater 1998, 5, 117.

20. Sova, M.; Raab, M.; Slizova, M. J Mater Sci 1993, 28, 6516.
21. Yang, Y.; Thompson, G.; Song, J.; Hiltner, A.; Baer, E. J Appl Polym Sci 2008, 112, 163.
22. Tang, H.; Hiltner, A.; Baer, E. Polym Eng Sci 1987, 27, 869.
23. Bartczak, Z. J Appl Polym Sci 2002, 86, 1396.
24. Pawlak, A. Polymer 2007, 48, 1397.
25. Bernal, T.; Masirek, R.; Hiltner, A.; Baer, E.; Piorkowska, E.; Galeski, A. J Appl Polym Sci 2006, 99, 597.
26. Chen, X.; Yoon, K.; Burger, C.; Sics, I.; Fang, D.; Hsiao, B.; Chu, B. Macromolecules 2005, 38, 3883.
27. Kohan, M. Nylon Plastics; Wiley: New York, 1973.
28. Feldman, A.; Gonzalez, M.; Wachtel, E.; Moret, M.; Marom, G. Polymer 2004, 45, 7239.
29. Na, B.; Zhang, Q.; Fu, Q.; Men, Y.; Hong, K.; Strobl, G. Macromolecules 2006, 39, 2584.
30. Wang, H.; Chum, S.; Hiltner, A.; Baer, E. J Polym Sci Part B: Polym Phys 2009, 47, 1313.
31. Li, D.; Garmestani, H.; Alamo, R.; Kalidindi, S. Polymer 2003, 44, 5355.
32. Dao, M.; Chollacoop, N.; Van Vliet, K.; Venkatesh, T. A.; Suresh, S. Acta Mater 2001, 49, 3899.
33. Al-Hussein, M.; Strobl, G. Macromolecules 2002, 35, 8515.
34. Hong, K.; Rastogi, A.; Strobl, G. Macromolecules 2004, 37, 10165.
35. Van Melick, H.; Govaert, L.; Meijer, H. Polymer 2003, 44, 2493.
36. Allan, P.; Bevis, M. Philos Mag 1980, 41, 555.